OPTICS

Synchronization of optical photons for quantum information processing

10.1126/sciadv.1501772

Kenzo Makino,[1] Yosuke Hashimoto,[1] Jun-ichi Yoshikawa,[1]* Hideaki Ohdan,[1] Takeshi Toyama,[1] Peter van Loock,[2] Akira Furusawa[1]*

A fundamental element of quantum information processing with photonic qubits is the nonclassical quantum interference between two photons when they bunch together via the Hong-Ou-Mandel (HOM) effect. Ultimately, many such photons must be processed in complex interferometric networks. For this purpose, it is essential to synchronize the arrival times of the flying photons and to keep their purities high. On the basis of the recent experimental success of single-photon storage with high purity, we demonstrate for the first time the HOM interference of two heralded, nearly pure optical photons synchronized through two independent quantum memories. Controlled storage times of up to 1.8 μs for about 90 events per second were achieved with purities that were sufficiently high for a negative Wigner function confirmed with homodyne measurements.

INTRODUCTION

Optical photons are a fundamental resource to encode flying quantum bits for quantum communication and computation. In particular, in linear-optics quantum information processing (*1*), universal two-qubit gates rely on nonclassical quantum interferences, where photons tend to bunch because of their bosonic nature. The elementary manifestation for this is the so-called Hong-Ou-Mandel (HOM) effect (*2*): when two indistinguishable single photons $|1, 1\rangle$ enter a balanced beam splitter, they bunch in either of the two output ports, resulting in a HOM state $|\mathrm{HOM}(\theta)\rangle = (|2, 0\rangle - e^{2i\theta}|0, 2\rangle)/\sqrt{2}$ with some relative phase θ. For large-scale quantum computation, many pure single photons must be available simultaneously at the input ports of large interferometric networks to apply the corresponding gate sequences at the same time on all the initial qubits. Numerous tests of the HOM effect have been performed over the past few decades, mainly to characterize single-photon sources, such as parametric down-converters (*3*, *4*), single neutral atoms (*5*, *6*), ions (*7*), atomic ensembles (*8*), quantum dots (*9*–*12*), and nitrogen vacancy centers in diamonds (*13*). However, the simultaneous occurrence of two single photons at a beam splitter has depended on a random coincidence between two independent statistical sources. One possible way toward scalability is to combine statistical photon sources with quantum memories (see Fig. 1), by which a photon is stored until the other photon becomes available as well (*14*, *15*). However, such quantum storage must not be at the expense of the single-photon purity. In fact, a fundamental change takes place when an ideal single-photon wave function (that is, an optical quantum oscillator mode in its first excited pure state) is mixed together with the vacuum wave function (corresponding to the unexcited ground state). If the vacuum fraction is larger than that of the single photon, the otherwise highly nonclassical, negative Wigner function of a single-photon state becomes positive. The Wigner function, representing the quantum state of a light field composed of one or more optical modes, is a quasi–probability distribution function for the modes' phase-space variables. The occurrence of a Wigner function with some negative values in phase space not merely indicates strong nonclassicality, but also is a necessary requirement to prevent the efficient simulation of a quantum computation by a classical computer (*16*–*18*). Only in two very recent experiments were optical single-photon states, which were sufficiently pure that they showed a negative dip in their Wigner functions (*16*), released in a controlled fashion (quasi–on demand) from a memory system based on optical cavities (*19*, *20*) and from another one based on atomic ensembles (*21*).

Here, we report the next significant step beyond this: the controlled HOM interference of two nearly pure photons that emerge from two independent quantum memories using the cavity-storage method (*19*, *20*). The resulting states still have single-photon purities that are higher than 0.5, which is sufficient for a negative Wigner function. Because of the memories, which use controlled storage times of up to 1.8 μs, the output HOM state can be synchronized (see Fig. 1B). Compared to previous research on atomic memories, the memory times of our all-optical system are of a similar order (*14*, *15*), but the purities of the synchronized photons are raised to an unprecedented, qualitatively different level. We believe that this controlled, almost on-demand demonstration of the HOM effect represents a breakthrough toward scaling up photonic quantum interference experiments, with direct applications in linear-optics quantum computation (*1*), quantum communication (*22*), and boson sampling (*23*).

Another important aspect of our approach, making it distinct from all postselective schemes based on particle-like click-by-click photon detections, is the characterization of the resulting HOM state from a wave-like perspective using homodyne measurements of field quadrature amplitudes. Here, we will show that a characteristic pattern in the wave basis survives even after active synchronization with quantum memories. Thus, reflecting the wave-particle duality, which is a fundamental feature of quantum mechanics, our demonstration looks at the famous HOM effect from a completely wave-like angle. This is not only of fundamental interest but also practically important for optical hybrid quantum information processing, where both continuous wave and discrete particle properties are exploited for quantum-state preparation, processing, and detection (*24*, *25*). Since its first demonstration (*2*), the HOM effect has always been expressed as a dip in the coincidence probability of photon detections at both output ports of the beam splitter. However, the HOM dip only reflects a particle-like aspect of the HOM state, in which photonic particle bunching becomes manifest.

[1]Department of Applied Physics, School of Engineering, The University of Tokyo, 7-3-1 Hongo, Bunkyo-ku, Tokyo 113-8656, Japan. [2]Institute of Physics, Johannes Gutenberg-Universität Mainz, Staudingerweg 7, 55099 Mainz, Germany.
*Corresponding author. Email: yoshikawa@ap.t.u-tokyo.ac.jp (J.Y.); akiraf@ap.t.u-tokyo.ac.jp (A.F.)

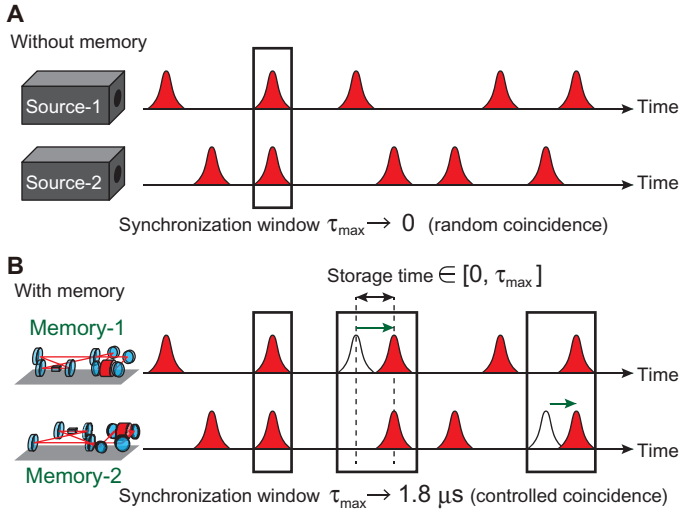

Fig. 1. Synchronization of optical photons. (**A**) Independent statistical photon sources without memories. (**B**) Independent photon sources with memories. τ_{max}, the maximum storage time. In principle, the synchronization window could be further increased beyond 1.8 μs; however, in our present performance of memories, this would be at the expense of the negativity of the Wigner function.

The more general, actual quantum nature of that prominent optical quantum state, such as quantum entanglement, cannot be revealed by correlation measurements in a fixed particle basis. The wave-basis image of the HOM state that we present here as a counterpart to the particle-basis HOM dip is a correlation pattern that is similar to a four-leaf clover that vanishes and reappears depending on the relative phase θ (*26*, *27*). The phase-dependent pattern is actually sufficient to fully characterize the HOM state and to obtain its density matrix (*28*). However, the pattern is very fragile against optical losses and detection noises mostly because the homodyne detection is sensitive to vacuum fluctuations. This is unlike the HOM dip whose shape is, in principle, unchanged even for large optical losses. Therefore, to observe the phase-sensitive clover pattern, highly pure single photons must be prepared simultaneously and detected with very low noise homodyne detectors, which became possible only very recently (*19*–*21*, *26*, *27*).

RESULTS

Synchronization of single photons and its performance

Our experimental setup is schematically shown in Fig. 2A, where each of the two single-photon sources is enclosed by a memory system (Memory-1 or Memory-2) that is composed of two concatenated cavities (*19*, *20*). Single-photon wave packets are almost identical for various storage times between the two sources, as shown in Fig. 2B. In the HOM interference experiment, the first photon that is heralded earlier on either side of the input ports is kept until the second photon is heralded later on the other side. Then, the two photons are released simultaneously when the difference between their heralding times is shorter than 2 μs. This time difference, corresponding to the storage time of the first photon, was recorded for each event together with the homodyne outcomes. We acquired two-mode quadrature data for 390,636 events. This large number of events was acquired within only 3 hours. To observe the dependence on the maximum storage time τ_{max}, we analyzed those events associated with a storage time between 0 and τ_{max}. Figure 2C shows the individual input single-photon purities, calculated with the maximum likelihood method (*28*) for each τ_{max}. Although the single-photon purities degrade for longer storage times, according to a finite memory lifetime, the purities were kept above the 0.5 limit of the Wigner function negativity condition for up to about 1.8 μs, which corresponds to about 90 events per second. The coherence time of the wave packets for the 0.5 criteria without synchronization is estimated at 72 ns, and thus, the memory enhancement in the event rate can be calculated as a factor of 25. Further information is given in the Supplementary Materials.

HOM state in the wave basis

Let us now discuss the image of the HOM state in the wave basis, as shown in Fig. 3. Theoretically, vacuum $|0\rangle$, single-photon $|1\rangle$, and two-photon $|2\rangle$ states have one, two, and three peaks in their quadrature distributions, respectively, and thus, the two-dimensional distributions of the separable states $|2, 0\rangle$ and $|0, 2\rangle$ look like those in Fig. 3 (A and B, respectively). When $|2, 0\rangle$ and $|0, 2\rangle$ are coherently superimposed to obtain the HOM state, $|\mathrm{HOM}(\theta)\rangle = (|2, 0\rangle - e^{2i\theta}|0, 2\rangle)/\sqrt{2}$, the probability amplitudes at the origin destructively or constructively interfere depending on θ (*26*, *27*). As a result, the remaining distribution patterns are the four-leaf clover for θ = 0° (Fig. 3C) and a concentric pattern for θ = 90° (Fig. 3D).

These characteristic distribution patterns are indeed observed in our experiment by homodyne detections. In Fig. 4 (A and B), the distributions of the output for θ = 0° and 90° are shown, together with the individual histograms of the single-mode quadratures. These are the results for a τ_{max} of 400 ns, as a typical example. The output barely exhibits side fringes reflecting a large two-photon component (top and right panels in Fig. 4, A and B). The two-mode distributions of the output completely change depending on θ. The four-leaf clover is most pronounced at θ = 0°, whereas the clover totally disappears at θ = 90°, as expected from Fig. 3 (C and D) (*26*, *27*). These distributions are totally different from that of the case without synchronization (Fig. 4C). The results here are only particular examples, and the full results are presented in the Supplementary Materials, together with those for the phase-independent input state.

Quantum-state tomography

Thus far, we have discussed the relative phase θ of the HOM state $|\mathrm{HOM}(\theta)\rangle = \hat{U}(\theta)|\mathrm{HOM}(0)\rangle$, where $\hat{U}(\theta) = e^{i\theta\hat{a}_2^\dagger\hat{a}_2}$ is the phase-shift operator acting on the second mode. From a different viewpoint, this can be reinterpreted as a phase shift of the measured quadratures $\langle x_1, x_2|\hat{U}(\theta)$ for the fixed state $|\mathrm{HOM}(0)\rangle$, because $\Pr(x_1, x_2) = |\langle x_1, x_2|\hat{U}(\theta)|\mathrm{HOM}(0)\rangle|^2$. In the latter interpretation, the wave-basis two-mode distributions with various measurement phases contain the complete information for estimating the quantum state (*28*). In Fig. 4D, the density matrix of the output state $\hat{\rho}_{out}$ is shown in the number basis. The ideal density operator of the HOM state is $\hat{\rho}_{HOM} = |\mathrm{HOM}(0)\rangle\langle\mathrm{HOM}(0)| = \frac{1}{2}(|0, 2\rangle\langle 0, 2| + |2, 0\rangle\langle 2, 0| - |0, 2\rangle\langle 2, 0| - |2, 0\rangle\langle 0, 2|)$, and this structure also becomes apparent in the experimental output state $\hat{\rho}_{out}$: the diagonal elements of $|2, 0\rangle\langle 2, 0|$ and $|0, 2\rangle\langle 0, 2|$ indicate the photon bunching effect on the $|1, 1\rangle\langle 1, 1|$ component of the input, whereas the presence of the off-diagonal, negative elements of $|0, 2\rangle\langle 2, 0|$ and $|2, 0\rangle\langle 0, 2|$ proves that the bunched components are quantum-mechanically superimposed rather than classically, incoherently mixed. These off-diagonal elements are (necessary and) sufficient for the entanglement

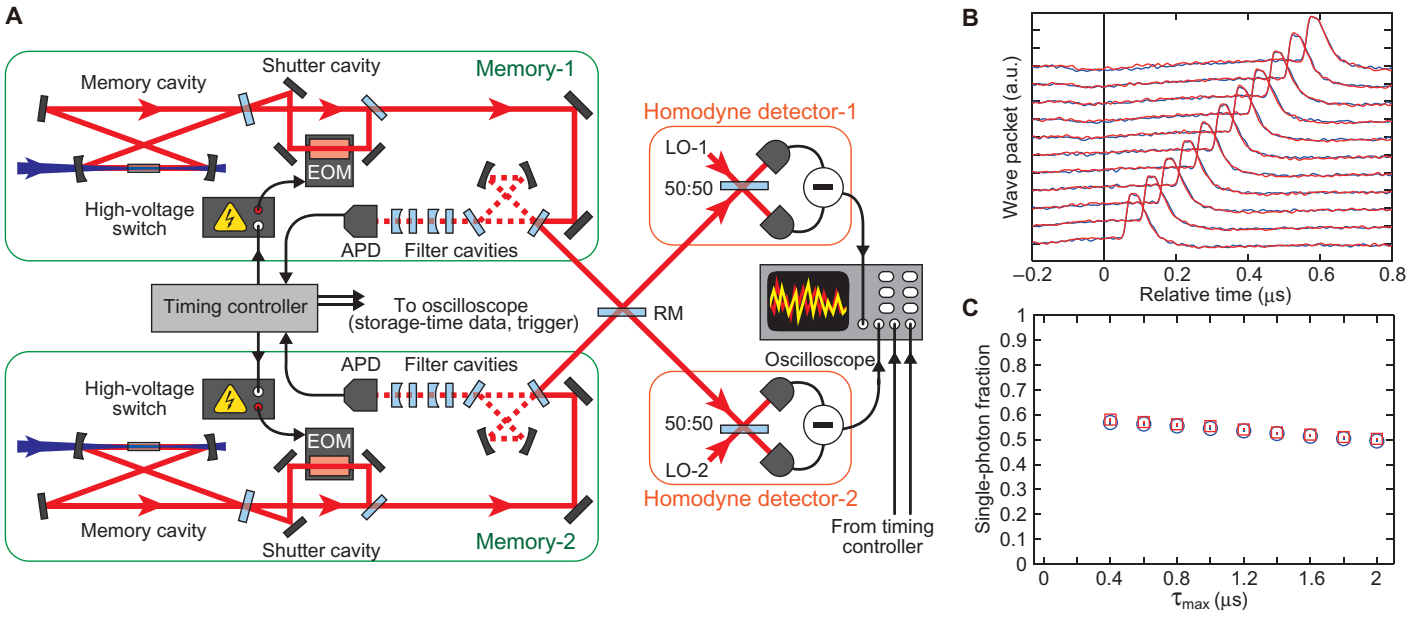

Fig. 2. Experimental setup and characterization. (**A**) Experimental setup. EOM, electro-optic modulator; APD, avalanche photodiode; LO, local oscillator; RM, replaceable mirror. (**B**) Experimentally estimated wave packets of single photons released from Memory-1 (blue traces) and Memory-2 (red traces) after various fixed storage times. The plots are vertically shifted according to the storage times from 0 to 500 ns by 50-ns steps. The horizontal axis is the time relative to each heralding event. The intrinsic delay in the memory release is about 50 ns. a.u., arbitrary units. (**C**) Experimental single-photon purities after the synchronization without any correction of detection inefficiencies. Circles and squares are $\langle 1|\mathrm{Tr}_k\{\hat{B}^\dagger\hat{\rho}_{out}\hat{B}\}|1\rangle$ for Memory-1 ($k = 2$) and Memory-2 ($k = 1$), respectively. They are calculated from the output with the numerical inverse of the balanced beam splitter $\hat{B}$. Error bars are from ±0.007 to ±0.003.

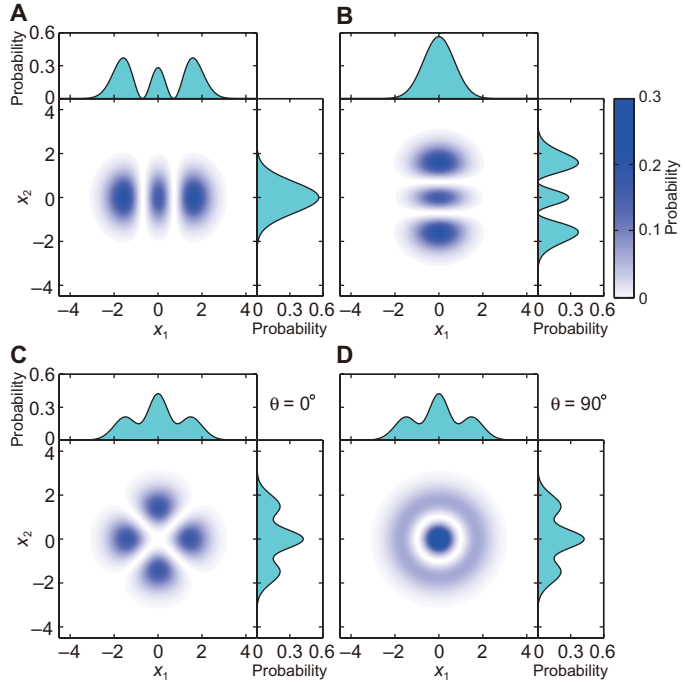

Fig. 3. Theoretical two-mode quadrature distributions in the ideal cases. (**A**) $|2, 0\rangle$ state. (**B**) $|0, 2\rangle$ state. (**C** and **D**) Coherent superposition $|\mathrm{HOM}(\theta)\rangle$ for θ = 0° (C) and for θ = 90° (D). The probability amplitudes at the origin interfere destructively (C) or constructively (D). The marginal distributions are also shown in the top and right panels.

between the two output modes. Quantitatively (*29*), a logarithmic negativity $\log_2||\hat{\rho}_{out}^{T_1}|| = 0.37 \pm 0.01$ is obtained, whereas in the ideal case, $\log_2||\hat{\rho}_{HOM}^{T_1}|| = 1$. Moreover, the strong nonclassicality of the output state is evident from its negative Wigner function $W(x_1, p_1, x_2, p_2)$. The cross section $W(x_1, 0, x_2, 0)$ shown in Fig. 4E has negative values in a structure reflecting the four-leaf clover pattern. The density matrix of the input and a further evaluation can be found in the Supplementary Materials.

DISCUSSION

We have experimentally demonstrated the famous HOM interference effect in a way that is potentially scalable toward large-scale quantum information processing. To achieve this, two nearly pure single photons enter a beam splitter almost on demand after their synchronized release from two independent optical (cavity-based) quantum memories. We have also shown the wave-like aspect of the resulting HOM state via homodyne detections, characterized by a phase-dependent appearance of a four-leaf clover pattern. The quality of the states is sufficient to exhibit a negative Wigner function and entanglement even after memory storage. The HOM state interpreted as a NOON state (*30*) is also potentially useful in quantum metrology and sensing.

A current limitation of our approach is the occurrence of multiphoton terms from each source, accompanied by multiple photons in the corresponding heralding lines. This limitation could be overcome in the future by using photon number–resolving detectors with high quantum efficiency (*31*) and discarding events when multiphoton states are heralded (*32*, *33*).

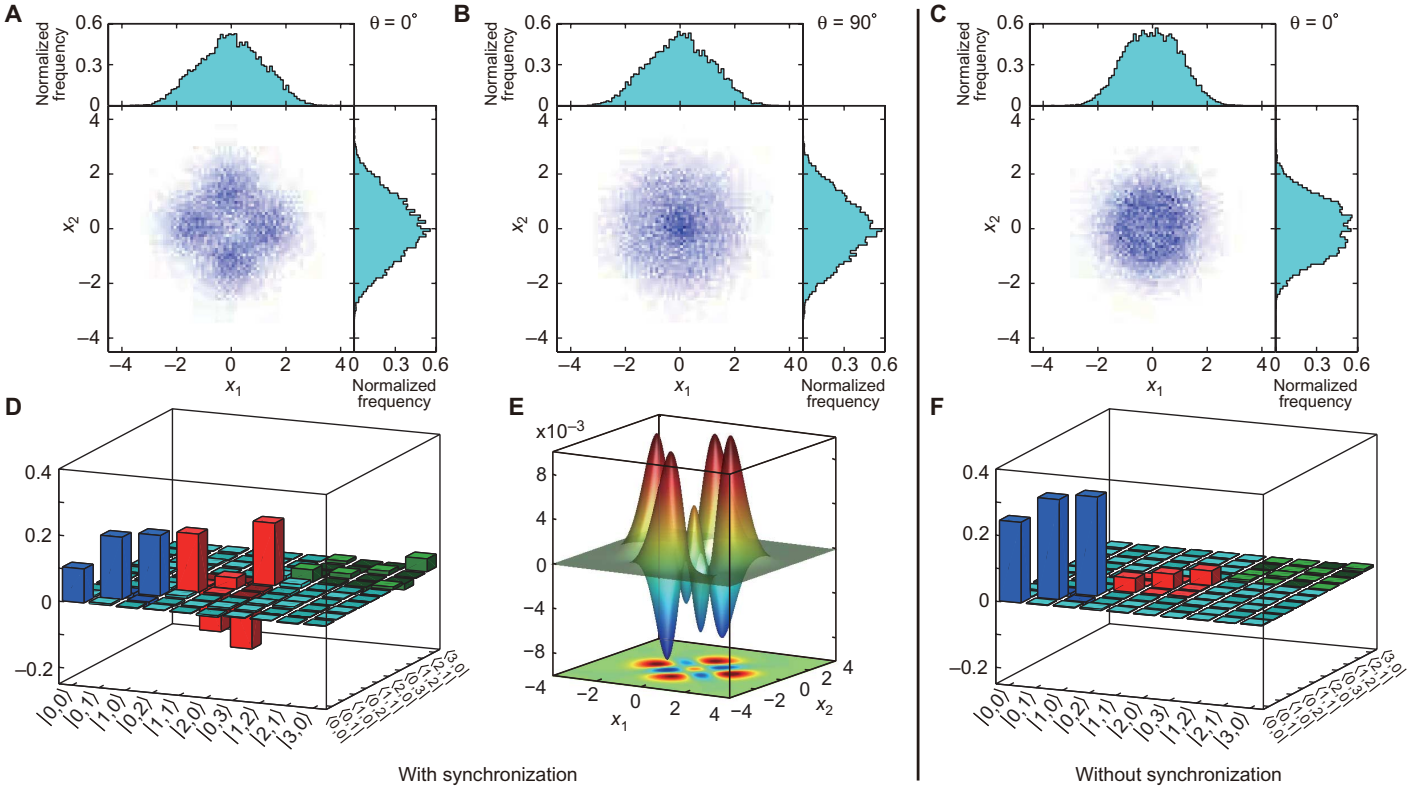

Fig. 4. Experimental outputs. (**A** and **B**) Experimental quadrature distributions of the output state after the synchronization for θ = 0° (A) and for θ = 90° (B). (**C**) Experimental distribution without synchronization for θ = 0°. (**D**) Density matrix of the output state after synchronization. The imaginary part of the density matrix is omitted because it is negligibly small; it can be found in the Supplementary Materials. (**E**) Cross section of the output Wigner function. (**F**) Density matrix of the output without synchronization.

MATERIALS AND METHODS

Working principle of the memory systems

The individual single-photon creations correspond to an ordinary quantum optical heralding scheme, where photons are probabilistically but simultaneously produced in pairs by nonlinear optical effects and one photon serves as the herald of the other (*16*). Single-photon sources based on such nonlinear optical effects have good controllability of the wavelength unlike other on-demand–type sources. The special interference inside the concatenated cavities ensures that the photon to be measured is released outside, whereas the photon to be prepared stays inside. After heralding, the stored single photon is released on demand by rapidly switching the cavity resonance via an electro-optic effect (*19*, *20*), which is also different from a simple storage-loop switching scheme (*34*). Formally, the weakly squeezed two-mode squeezed states from our nonlinear optical photon-pair source are equivalent to the initial spin-light entangled states in the Duan-Lukin-Cirac-Zoller (DLCZ) quantum repeater scheme, where the collective spin mode belongs to an atomic ensemble (*21*, *22*, *35*). The mechanism for a heralded loading of each memory in our all-optical scheme is therefore also analogous to DLCZ, though the information about which memory contains a photon is erased in DLCZ through an additional beam splitter in front of the two detectors. Our scheme, of course, can be easily adapted to such applications.

In the experiment, the memory cavity has a length of 1.4 m and contains the optical nonlinear medium of a periodically poled $KTiOPO_4$ crystal with a length of 10 mm. The shutter cavity has a length of 0.7 m and contains the electro-optic modulator of an $RbTiOPO_4$ crystal with an aperture size of 4 mm × 4 mm.

Preliminary experiment

We tested the performance of the individual memory systems by using a highly reflective mirror as the replaceable mirror in Fig. 2A. For both input ports, we estimated the wave packets of the released single photons for various fixed storage times after heralding (*19*, *20*, *36*). Figure 2B shows the longitudinal modes of the released wave packets in the time domain, vertically shifted depending on the corresponding storage times. It can be confirmed that the single-photon wave packets are correctly shifted by the memories without deformation and also that the wave packets from the two independent memories are almost identical. This sameness (indistinguishability) of the wave packets is critical for the HOM interference effect.

HOM interference experiment

We synchronized the photon sources and then obtained an output HOM state. The storage time of each event was recorded together with the homodyne outcomes. The single-heralding event rates were about 3200 counts per second (cps) for both Memory-1 and Memory-2, whereas the double-heralding event rate was about 90 cps with a maximum waiting time of 1.8 μs. This value agrees well with the theoretical prediction when a duty cycle of 40% is taken into account. We obtained 10,851 data points for each of the 36 combinations mentioned below, whereas 20,000 data points for vacuum fluctuations were used as a

reference. The actual single-photon emission rate corresponds to the product of the single-heralding event rate and the single-photon purity, whereas the actual double-emission rate corresponds to the product of the double-heralding event rate and the $|1, 1\rangle\langle 1, 1|$ component of $\hat{\rho}_{in}$. If we do not restrict ourselves to the 0.5 purity criteria, larger τ_{max} values can further increase the actual double-emission rate.

To observe the phase-sensitive quantum correlations, we set the optical phases of the two measured quadratures (θ_1 and θ_2) independently to 0°, 30°, 60°, 90°, 120°, and 150°. The change of θ_1 and θ_2 is achieved experimentally by shifting the local oscillator phases. In total, there are 36 possible combinations tested. However, the two-mode quadrature distributions are almost identical for equal relative phases $\theta = \theta_1 - \theta_2$, reflecting the phase insensitivity of the input single-photon states (as for the individual results of the 36 combinations, see the Supplementary Materials). Therefore, we collected the results with the same relative phases in single scatterplots as shown in Fig. 4 (A and B) for $\theta = 0°$ and $\theta = 90°$, respectively. More details can be found in the Supplementary Materials.

SUPPLEMENTARY MATERIALS

Supplementary material for this article is available at http://advances.sciencemag.org/cgi/content/full/2/5/e1501772/DC1

Supplementary Methods

Supplementary Discussion

table S1. Overlap of the wave packets and purity for each wave packet.

fig. S1. Input characterization and dependence on the maximum storage time.

fig. S2. Wave functions and probability distributions.

fig. S3. Experimental two-mode quadrature distributions of the output state.

fig. S4. Experimental quadrature distributions of the input and output states.

fig. S5. Real and imaginary parts of the density matrices.

fig. S6. Cross sections of the two-mode Wigner functions.

Reference (*37*)

REFERENCES AND NOTES

1. E. Knill, R. Laflamme, G. J. Milburn, A scheme for efficient quantum computation with linear optics. *Nature* **409**, 46–52 (2001).
2. C. K. Hong, Z. Y. Ou, L. Mandel, Measurement of subpicosecond time intervals between two photons by interference. *Phys. Rev. Lett.* **59**, 2044–2046 (1987).
3. H. de Riedmatten, I. Marcikic, W. Tittel, H. Zbinden, N. Gisin, Quantum interference with photon pairs created in spatially separated sources. *Phys. Rev. A* **67**, 022301 (2003).
4. M. Tanida, R. Okamoto, S. Takeuchi, Highly indistinguishable heralded single-photon sources using parametric down conversion. *Opt. Express* **20**, 15275–15285 (2012).
5. T. Legero, T. Wilk, M. Hennrich, G. Rempe, A. Kuhn, Quantum beat of two single photons. *Phys. Rev. Lett.* **93**, 070503 (2004).
6. J. Beugnon, M. P. A. Jones, J. Dingjan, B. Darquié, G. Messin, A. Browaeys, P. Grangier, Quantum interference between two single photons emitted by independently trapped atoms. *Nature* **440**, 779–782 (2006).
7. P. Maunz, D. L. Moehring, S. Olmschenk, K. C. Younge, D. N. Matsukevich, C. Monroe, Quantum interference of photon pairs from two remote trapped atomic ions. *Nat. Phys.* **3**, 538–541 (2007).
8. T. Chanelière, D. N. Matsukevich, S. D. Jenkins, S.-Y. Lan, R. Zhao, T. A. B. Kennedy, A. Kuzmich, Quantum interference of electromagnetic fields from remote quantum memories. *Phys. Rev. Lett.* **98**, 113602 (2007).
9. C. Santori, D. Fattal, J. Vučković, G. S. Solomon, Y. Yamamoto, Indistinguishable photons from a single-photon device. *Nature* **419**, 594–597 (2002).
10. E. B. Flagg, A. Muller, S. V. Polyakov, A. Ling, A. Migdall, G. S. Solomon, Interference of single photons from two separate semiconductor quantum dots. *Phys. Rev. Lett.* **104**, 137401 (2010).
11. O. Gazzano, S. Michaelis de Vasconcellos, C. Arnold, A. Nowak, E. Galopin, I. Sagnes, L. Lanco, A. Lemaître, P. Senellart, Bright solid-state sources of indistinguishable single photons. *Nat. Commun.* **4**, 1425 (2013).
12. Y.-M. He, Y. He, Y.-J. Wei, D. Wu, M. Atatüre, C. Schneider, S. Höfling, M. Kamp, C.-Y. Lu, J.-W. Pan, On-demand semiconductor single-photon source with near-unity indistinguishability. *Nat. Nanotechnol.* **8**, 213–217 (2013).
13. H. Bernien, L. Childress, L. Robledo, M. Markham, D. Twitchen, R. Hanson, Two-photon quantum interference from separate nitrogen vacancy centers in diamond. *Phys. Rev. Lett.* **108**, 043604 (2012).
14. D. Felinto, C. W. Chou, J. Laurat, E. W. Schomburg, H. de Riedmatten, H. J. Kimble, Conditional control of the quantum states of remote atomic memories for quantum networking. *Nat. Phys.* **2**, 844–848 (2006).
15. Z.-S. Yuan, Y.-A. Chen, S. Chen, B. Zhao, M. Koch, T. Strassel, Y. Zhao, G.-J. Zhu, J. Schmiedmayer, J.-W. Pan, Synchronized independent narrow-band single photons and efficient generation of photonic entanglement. *Phys. Rev. Lett.* **98**, 180503 (2007).
16. A. I. Lvovsky, H. Hansen, T. Aichele, O. Benson, J. Mlynek, S. Schiller, Quantum state reconstruction of the single-photon Fock state. *Phys. Rev. Lett.* **87**, 050402 (2001).
17. A. Mari, J. Eisert, Positive Wigner functions render classical simulation of quantum computation efficient. *Phys. Rev. Lett.* **109**, 230503 (2012).
18. M. Schleier-Smith, H. Tanji-Suzuki, Viewpoint: Pure photons for quantum communications. *Physics* **7**, 6 (2014).
19. J. Yoshikawa, K. Makino, S. Kurata, P. van Loock, A. Furusawa, Creation, storage, and on-demand release of optical quantum states with a negative Wigner function. *Phys. Rev. X* **3**, 041028 (2013).
20. J. Yoshikawa, K. Makino, A. Furusawa, in *Engineering the Atom-Photon Interaction*. A. Predojević, M. W. Mitchell, Eds. (Springer, Cham, 2015), chap. 8.
21. E. Bimbard, R. Boddeda, N. Vitrant, A. Grankin, V. Parigi, J. Stanojevic, A. Ourjoumtsev, P. Grangier, Homodyne tomography of a single photon retrieved on demand from a cavity-enhanced cold atom memory. *Phys. Rev. Lett.* **112**, 033601 (2014).
22. N. Sangouard, C. Simon, H. de Riedmatten, N. Gisin, Quantum repeaters based on atomic ensembles and linear optics. *Rev. Mod. Phys.* **83**, 33–80 (2011).
23. S. Aaronson, A. Arkhipov, The computational complexity of linear optics, in *Proceedings of the ACM Symposium on Theory of Computing* (ACM, New York, 2011), pp. 333–342.
24. S. Takeda, T. Mizuta, M. Fuwa, P. van Loock, A. Furusawa, Deterministic quantum teleportation of photonic quantum bits by a hybrid technique. *Nature* **500**, 315–318 (2013).
25. Y. Miwa, J. Yoshikawa, N. Iwata, M. Endo, P. Marek, R. Filip, P. van Loock, A. Furusawa, Exploring a new regime for processing optical qubits: Squeezing and unsqueezing single photons. *Phys. Rev. Lett.* **113**, 013601 (2014).
26. Y. Hashimoto, K. Makino, J. Yoshikawa, H. Ohdan, P. van Loock, A. Furusawa, paper presented at Frontiers in Optics 2014 OSA, Tucson, AZ, FW4C.3 (paper online), October 2014.
27. J. Etesse, M. Bouillard, B. Kanseri, R. Tualle-Brouri, Experimental generation of squeezed cat states with an operation allowing iterative growth. *Phys. Rev. Lett.* **114**, 193602 (2015).
28. A. I. Lvovsky, M. G. Raymer, Continuous-variable optical quantum-state tomography. *Rev. Mod. Phys.* **81**, 299–332 (2009).
29. M. B. Plenio, Logarithmic negativity: A full entanglement monotone that is not convex. *Phys. Rev. Lett.* **95**, 090503 (2005).
30. T. Nagata, R. Okamoto, J. L. O'Brien, K. Sasaki, S. Takeuchi, Beating the standard quantum limit with four-entangled photons. *Science* **316**, 726–729 (2007).
31. D. Fukuda, G. Fujii, T. Numata, K. Amemiya, A. Yoshizawa, H. Tsuchida, H. Fujino, H. Ishii, T. Itatani, S. Inoue, T. Zama, Titanium-based transition-edge photon number resolving detector with 98% detection efficiency with index-matched small-gap fiber coupling. *Opt. Express* **19**, 870–875 (2011).
32. A. Ourjoumtsev, R. Tualle-Brouri, P. Grangier, Quantum homodyne tomography of a two-photon Fock state. *Phys. Rev. Lett.* **96**, 213601 (2006).
33. A. Zavatta, V. Parigi, M. Bellini, Toward quantum frequency combs: Boosting the generation of highly nonclassical light states by cavity-enhanced parametric down-conversion at high repetition rates. *Phys. Rev. A* **78**, 033809 (2008).
34. T. B. Pittman, J. D. Franson, Cyclical quantum memory for photonics qubits. *Phys. Rev. A* **66**, 062302 (2002).
35. L.-M. Duan, M. D. Lukin, J. I. Cirac, P. Zoller, Long-distance quantum communication with atomic ensemble and linear optics. *Nature* **414**, 413–418 (2001).
36. O. Morin, C. Fabre, J. Laurat, Experimentally accessing the optimal temporal mode of traveling quantum light states. *Phys. Rev. Lett.* **111**, 213602 (2013).
37. M. R. Ray, S. J. van Enk, Verifying entanglement in the Hong-Ou-Mandel dip. *Phys. Rev. A* **83**, 042318 (2011).

Acknowledgments

Funding: This work was partly supported by the Project for Developing Innovation Systems and the Advanced Photon Science Alliance (commissioned by the Ministry of Education, Culture, Sports, Science, and Technology of Japan), Grants-in-Aid for Scientific Research of the Japan Society for the Promotion of Science (JSPS), the Core Research for Evolutional Science and Technology of the Japan Science and Technology Agency, and the Strategic Information and Communications R&D Promotion Programme of the

Ministry of Internal Affairs and Communications of Japan. P.v.L. was supported in Germany by Qcom (Federal Ministry of Education and Research) and HIPERCOM [ERA-Net CHIST-ERA (European Coordinated Research on Long-term Challenges in Information and Communication Sciences & Technologies ERA Net)]. K.M. acknowledges support from JSPS. **Author contributions:** J.Y. conceived the experiment. K.M., Y.H., J.Y., H.O., and T.T. conducted the experiment, which was supervised by A.F. K.M. mainly designed the setup. K.M., Y.H., J.Y., and T.T. acquired and analyzed the data. K.M., J.Y., and A.F. discussed with P.v.L. the experimental results and future applications. K.M., J.Y., P.v.L., and A.F. prepared the manuscript with assistance from all other co-authors. **Competing interests:** The authors declare that they have no competing interests. **Data and materials availability:** All data needed to evaluate the conclusions in the paper are present in the paper and/or the Supplementary Materials. Additional data related to this paper may be requested from the authors.

Submitted 5 December 2015
Accepted 28 April 2016
Published 27 May 2016
10.1126/sciadv.1501772

Citation: K. Makino, Y. Hashimoto, J. Yoshikawa, H. Ohdan, T. Toyama, P. van Loock, A. Furusawa, Synchronization of optical photons for quantum information processing. *Sci. Adv.* **2**, e1501772 (2016).

Synchronization of optical photons for quantum information processing

Kenzo Makino, Yosuke Hashimoto, Jun-ichi Yoshikawa, Hideaki Ohdan, Takeshi Toyama, Peter van Loock and Akira Furusawa

Sci Adv **2** (5), e1501772.
DOI: 10.1126/sciadv.1501772